Supplementary Information:

Direct observation of the Mottness and p-d orbital hybridization in monolayer α-$RuCl_3$

Zhongjie Wang, [1] Lu Liu, [1, 2] Haoran Zheng, [1] Meng Zhao, [1] Ke Yang, [1, 2] Chunzheng Wang, [1] Fang Yang, [3,4] Hua Wu, [1,2,5,6*] Chunlei Gao[1,3,4,5,6,7#]

1 State Key Laboratory of Surface Physics and Department of Physics, Fudan University, Shanghai 200433, China

2 Laboratory for Computational Physical Sciences (MOE), Fudan University, Shanghai 200433, China

3 Institute for Nanoelectronic Devices and Quantum Computing, Fudan University, Songhu Rd. 2005, Shanghai 200438, China

4 Zhangjiang Fudan International Innovation Center, Fudan University, Shanghai 201210, China

5 Shanghai Qi Zhi Institute, Shanghai 200232, China

6 Collaborative Innovation Center of Advanced Microstructures, Nanjing University, Nanjing 210093, China

7 Shanghai Research Center for Quantum Sciences，Shanghai 201315，China

*Corresponding authors: *wuh@fudan.*edu.cn, #clgao@fudan.edu.cn

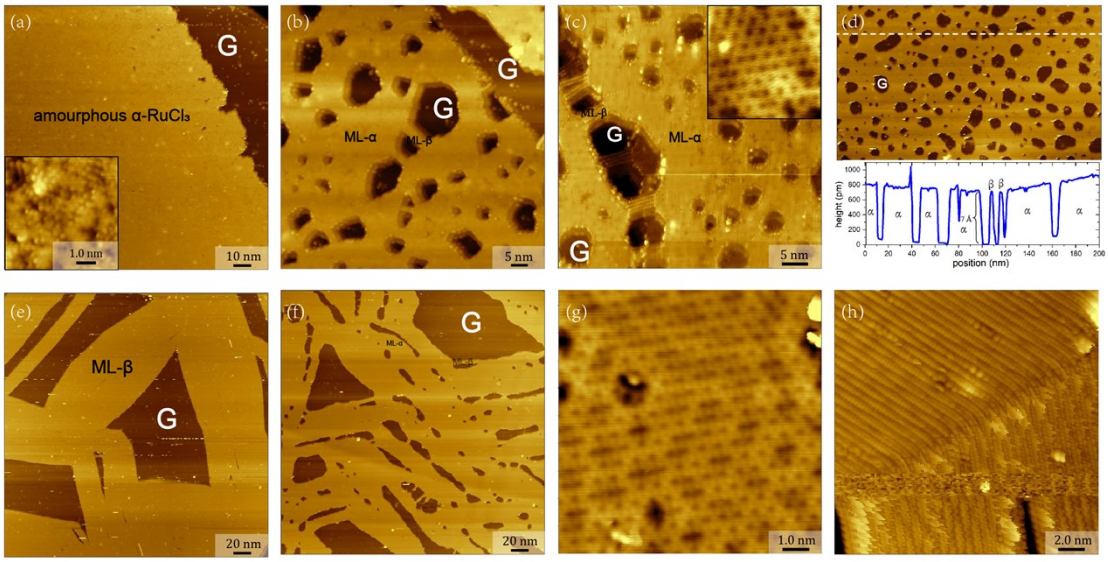

Figure. S1 Detailed topographic characterization of the sample before and after annealing. (a) STM image of amorphous monolayer α-$RuCl_3$ before annealing. The inset shows the microscopic disordered structure. (b-d) topographic images illustrate the transformation of the original amorphous α-$RuCl_3$ island into orderliness. The inset of (c) shows the zoomed-in image of orderly α-$RuCl_3$. (d) shows the morphology and the height profile along the dashed white line. (e) STM image of monolayer β-$RuCl_3$ before annealing. (f-g) The topographic images of the annealed monolayer $RuCl_3$ transformed from the β-phase precursor.

Only monolayer β-$RuCl_3$ and amorphous α-$RuCl_3$ are deposited at the preliminary growth before annealing, as Fig. S1(a, e) display the STM topography. The graphite substrate and α-/β-monolayer are labeled in the Fig. S1. The β- and amorphous α-monolayer can both be structurally transformed into crystalline monolayer α-$RuCl_3$ in a thermal triggered manner. Fig. S2(b-d) profile the monolayer $RuCl_3$ evolving from the initial amorphous α-phase with a brand-new appearance after annealing. The entire monolayer amorphous α-island contracts and rips into a cheese-like appearance with the β-chains bridging between the domains of α-$RuCl_3$. The annealed monolayer becomes compact and crystalized, and interestingly, there are β-bridges pulled out from the α-$RuCl_3$ domains during the contraction. Although there is double image in Fig. S2(b,c) due to the blunt tip apex, they provides high resolution to identify the crystal texture of α- and β-$RuCl_3$. The size of the monolayer α-flake is of several hundred nanometers, with a typical span of 200-800 nm depending on the domain size of initial amorphous flake. Fig. S1(d) shows the morphology and the height data along the white dashed line which intersects across both phase of $RuCl_3$ monolayer. The height of two phases of $RuCl_3$ monolayer are both 7Å. The pure β-monolayer in Fig. S1(e) would be transformed into a mixture of α- and β-$RuCl_3$ during annealing, as seen in Fig. S1(f) showing the topography of post-annealing. The size of α-patch is narrowed down to tens of nanometers in this case. The edge of α-monolayer is smooth and curved, while the β-monolayer has a straight one. The detailed images of Fig. S1(g, h) are extracted from the sample of Fig. S1(f) and illustrate the coexistence of both phases.

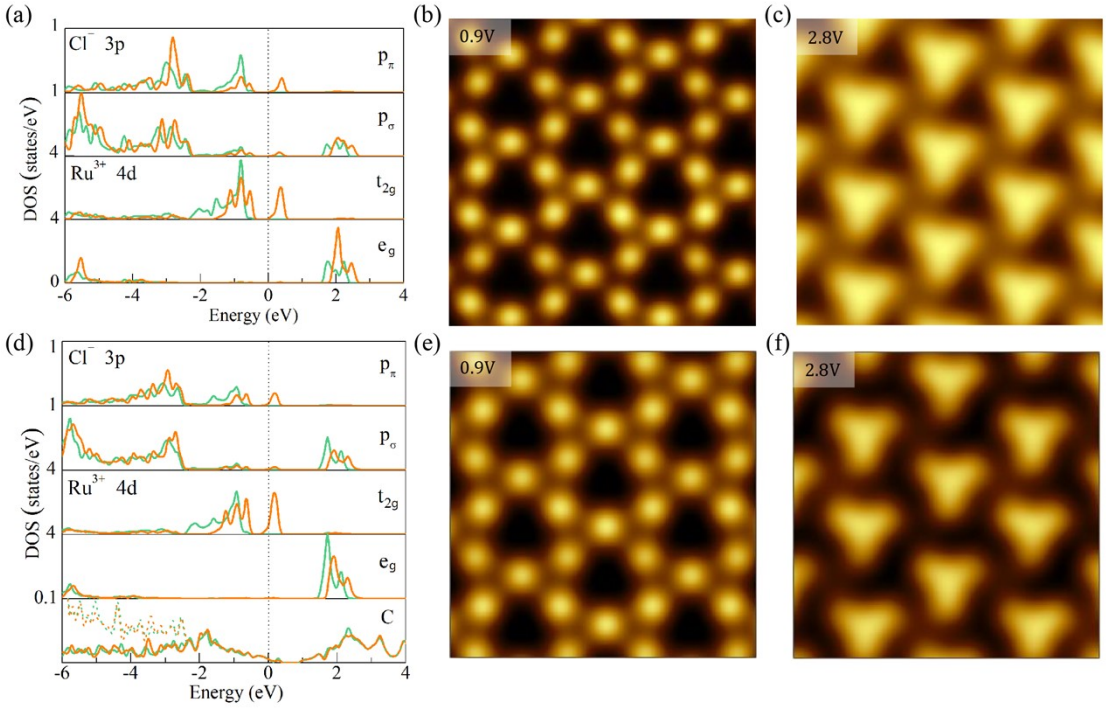

Figure. S2 The PDOS results and STM image simulations of the bare strained α-$RuCl_3$ monolayer (a-c) and the α-$RuCl_3$/graphene heterostructure (d-f). For PDOS results (a, d) by LSDA+SOC+U, the green (orange) curves describe the majority (minority) spins, and the dash (solid) curves in the bottom panel of (d) stand for total (p_z) states of C atoms. The Fermi level is set at zero energy. The STM simulations at 0.9 V (b, e) and 2.8 V (c, f) give the representative "Kagome-like" and triangular STM patterns, respectively.

Considering possible proximity effect by graphene substrate, we also carry out calculations for α-$RuCl_3$/graphene heterostructure. The bilayer supercell is constructed by stacking the strained α-$RuCl_3$ monolayer ($\frac{3}{2} \times \frac{3}{2}$) on graphene ($\sqrt{19} \times \sqrt{19}$). The PDOS results for the bare α-$RuCl_3$ monolayer and α-$RuCl_3$/graphene heterostructure are shown in Fig. S2 (a, d) respectively. We find that after contacting with graphene, the Fermi level of α-$RuCl_3$ slightly shifts up of ~ 0.05 eV using Ru 1s core state as energy reference, which indicates a minor electron transfer from graphene to α-$RuCl_3$ and is consistent with previous studies[1-4]. Moreover, our results show that comparing to the bare strained lattice, the lightly electron doped α-$RuCl_3$ has the almost unchanged orbital configurations. For Ru^{3+} (t_{2g}^5) ions, the local octahedral crystal field leads to the t_{2g}-e_g splitting of ~ 2 eV, and the partially occupied minority spin t_{2g} bands give rise to an ~ 0.6 eV Mott gap. Besides, Cl 3p valence bands lie below -2 eV, and Ru-Cl orbital hybridization yields Cl 3p antibonding states above -2 eV, where p_π dominates in -2.0 to 1.5 eV energy range by t_{2g}-p_π hybridization and p_σ dominates in 1.5 to 4 eV via e_g-p_σ one. Given that the STM patterns are mainly contributed by 3p orbitals of the upper

Cl ions, the results of STM simulations are slightly changed after considering the graphene substrate as shown in Fig. S2(b, c, e, f). The main conclusions remain valid as the "Kagome-like" lattice at 0.9V and the triangular lattice at 2.8V with or without the graphene substrate.

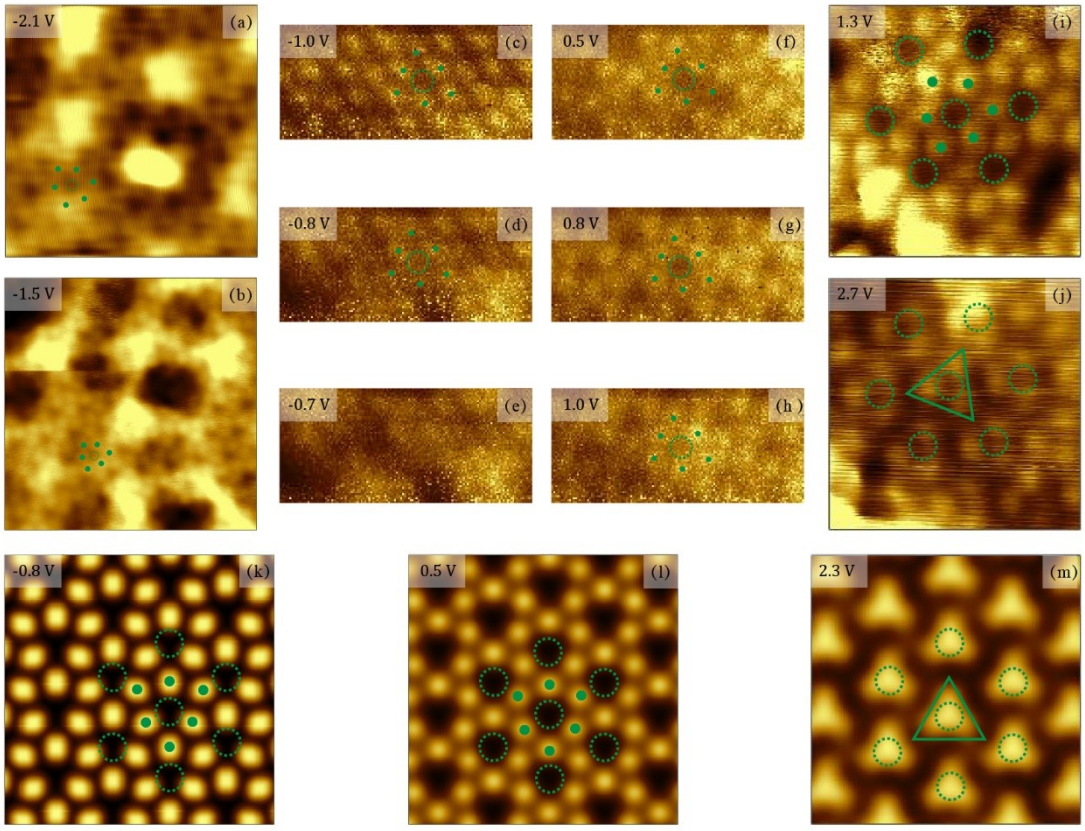

Figure. S3 Comparison between experimental and computational LDOS maps. (a-j) are the experimental dI/dV maps recorded at indicated bias voltage. Among them, (a,b), (c-h) and (i,j) are three sets of LDOS maps, each set is recorded with the same tip apex at the same sample area. In those images, the six green solid dots or the green triangle together with central dashed circles signpost the basic unit constructing the orbital patterns. In (i,j), the six dashed circles mark the same positions of the sample in real space between the two images. (k-m) are the simulated LDOS images at indicated bias, where the orbital pattern changes from (l) to (m) as the energy rises form t_{2g}-p_{π} range to e_g-p_{σ} range. Referring to the relative position between the pattern and the six dashed circles in images (i,j,l,m), the "Kagome-like" pattern will transform into the triangular lattice of trimers with six bright protrusions of the initial irregular hexagon clustering in a group of three, in a three-in and three-out manner.

Fig. S3 is the comparison between experimental and simulated local density of states (LDOS) maps of different energy. Fig. S3(a-j) are experimentally resolved dI/dV maps recorded at indicate bias voltages traversing the t_{2g} and e_g energy range. Fig. S3(k-m) are the corresponding calculated LDOS maps which show consistent orbital texture to the experimental dI/dV maps. Basically, the electronic patterns switch between the "Kagome-like" lattice and the triangular arranged trimers,

depending on whether the bias locates in the range of t_{2g}-p_π levels or e_g-p_σ levels. One can notice that there is heterogeneous corrugation presented in the experimental dI/dV maps. We attribute it to the inhomogenous strain in the monolayer, which leads to a heterogenous disproportion of t_{2g} energy levels with the manifestation of the spatially irregular modulation (which is very apparent in Fig. S2(a,b)). While this disproportional modulation is much weaker in the STM topographic data (Fig. 3) since that the corrugation in the topographic data come from the overall electronic states and this heterogenous disproportion of the t_{2g} energy levels is integrated out energetically.

(1) S. Biswas, Y. Li, S. M. Winter, J. Knolle, and R. Valentí, *Electronic Properties of α−$RuCl_3$ in Proximity to Graphene*, Phys. Rev. Lett. **123**, 237201 (2019).

(2) E. Gerber, Y. Yao, T. A. Arias, and E.-A. Kim, *Ab Initio Mismatched Interface Theory of Graphene on α−$RuCl_3$: Doping and Magnetism*, Phys. Rev. Lett. **124**, 106804 (2020).

(3) Boyi Zhou, J. Balgley, P. Lampen-Kelley, J.-Q. Yan, D. G. Mandrus, and E. A. Henriksen, *Evidence for charge transfer and proximate magnetism in graphene–α−RuCl3 heterostructures*, Phys. Rev. B **100**, 165426 (2019).

(4) Y. Kim, J. Kim, D. Weber, T. Taniguchi, K. Watanabe, N. Park, B. Lotsch, J. H. Smet, M. Burghard, and K. Kern, *Spin-Split Band Hybridization in Graphene Proximitized with α-RuCl3 Nanosheets*, Nano Lett. **19**, 4659 (2019).